X-645-72-176
PREPRINT

NASA TM X-65904

THE RING CURRENT

MASAHISA SUGIURA

MAY 1972

GSFC
GODDARD SPACE FLIGHT CENTER
GREENBELT, MARYLAND

THE RING CURRENT

Masahisa Sugiura
NASA-Goddard Space Flight Center, Laboratory for Space Physics
Greenbelt, Maryland 20771

May 1972

To appear in the Proceedings of the Symposium on "Critical Problems of the Magnetosphere Physics," Fifteenth Plenary Meeting of COSPAR, 10-24 May 1972, Madrid, Spain

THE RING CURRENT

Masahisa Sugiura
NASA-Goddard Space Flight Center, Laboratory for Space Physics,
Greenbelt, Maryland 20771

Abstract. The topology of ΔB (i.e., the observed scalar magnetic field intensity minus a scalar reference field intensity) in the magnetosphere has been established by the Rb magnetometer observations on OGO's 3 and 5. This ΔB topology provides a convenient framework, on the basis of which the complex features found by the earlier magnetic field observations made by Explorers 10, 12, 14, 26 and Electron 2 can be re-interpreted to fit to a unified simple picture of the magnetospheric field distortions including the inflation of the equatorial magnetosphere by the ring current. It is proposed that the quiet-time ring current consists of two parts, the inner ring current imbedded deeply inside the plasmapause and the outer ring current flowing in the plasma sheet. The source of the inner ring current appears to be trapped protons with energies 100 kev to several hundred kev having their peak intensity at 3 to 4 R_e, originally observed by Davis and Williamson (1963). The dominant source of the outer ring current is the population of protons with energy near 50 kev in the plasma sheet, as in Frank's (1967) model for the 'extraterrestrial ring current'. The outer ring current is an innermost part of the tail current, and the inner ring current is its earthward extension. The plasma pressure is nearly continuous from the plasma sheet to the inner current ring region. When plasma sheet moves inward during a substorm, the plasma pressure increase is directly conveyed to inside the plasmasphere and intensifies the inner ring current.

Introduction

The ring current at quiet and disturbed times has been an evasive subject both observationally and theoretically. The primary objectives of this review are to present a comprehensive picture of the distortion of the magnetosphere relative to the ring current and to convey the reasoning for the necessity of modifying the concept of the ring current.

Observations of the ring current field in the magnetosphere conducted up to about 1964 have been reviewed by Heppner (1967). For theoretical developments concerning the ring current, see, for instance, reviews by Chapman (1963) and Akasofu (1966). Discussions in the recent years have centered around the asymmetric (or partial) ring current which was first envisioned by Fejer (1961). On the basis of ground observations Akasofu and Chapman (1964) and Cummings (1966) concluded that the ring current grows asymmetrically with a maximum growth in the afternoon to evening sector in its developing stage. Parker (1966) presented a theory of such a partial ring current. Cahill (1966) confirmed the asymmetric development of the ring current by the Explorer 26 observations. Coleman and Cummings (1968) showed an example in which the storm field variations at ATS 1 are similar to those on the ground, indicating that the source is beyond 6.6 R_e. Very recently Cahill (1972) has presented results obtained by Explorer 45 during the December 16-18, 1971 storm, which are similar to his earlier observations.

The magnetic field observations on OGO's 3 and 5 had several unique features that are particularly suited for the reliable survey of the magnetospheric field. First, these observations have provided a very wide coverage over the several years of operation from the equatorial to the polar regions and from about 2 to 24 R_e in geocentric distance. Secondly, the Rb magnetometers gave very accurate scalar field measurements in the range from a few γ to several thousand γ. Thirdly, the GSFC fluxgate magnetometer on OGO 5 had high saturation points of about $\pm$ 4000γ along each axis. The discussions to be given in this paper and the conclusions drawn therefrom are largely the products of these factors.

ΔB Distribution in the Magnetosphere

For a proper understanding of the field distortions due to the ring current it is necessary to describe the ΔB distribution in the magnetosphere based on the Rb magnetometer observations on OGO's 3 and 5, where ΔB is the observed scalar field minus a scalar reference field (see Sugiura et al., 1971, for details). Figure 1 shows the ΔB contours in the noon-midnight meridian under magnetically quiet conditions as represented by Kp = 0-1. Dipole latitude and dipole local time are used in this presentation. The OGO 3 observations that were reactivated from February 1971 to February 1972 have provided data in the polar cap magnetosphere. It is important to observe the topology of ΔB. In this meridian plane the magnetosphere can be divided into four regions: (A) the equatorial -ΔB region encircling the earth, (B) the nightside +ΔB region outside Region A, consisting of the northern and southern branches adjoining at the dipole equator, (C) the two separate -ΔB regions in the outer magnetosphere in the noon meridian at mid to high latitudes, one in each hemisphere, and (D) the +ΔB region in the outer magnetosphere near the dipole equator in the noon meridian. Region D is topologically connected to Region B as will become clear in Figure 2; Region D is distinguished from Region B for the sake of convenience. The minimum values of ΔB in Region A are $\leq -35\gamma$ and are near 3 R_e in the noon and midnight meridians. The area of Region A in the noon half-plane is very much smaller than the corresponding area in the midnight half-plane. The maxima of ΔB in Region B are at midlatitudes and are about 25 to 30γ. A detailed study has shown that the north-south asymmetry seen in Figure 1 comes from seasonal effects.

As we go around the earth from the noon meridian toward the dawn and dusk sides, Region A expands and Region C diminishes in size, and the ΔB distribution in the dawn-dusk meridian plane becomes as shown in Figure 2, which is also for Kp = 0-1. Here we only see continuations of Regions A and B of Figure 1; Region D has merged into Region B, and Region C has completely disappeared. It is not certain if the dawn-dusk difference in the ΔB minimum in Region A is real, because ΔB is a time-varying quantity. However, the tendency that the contours are more stretched outward near the dipole equator on the dusk side than on the dawn side is probably real as the same tendency is seen also for more disturbed conditions. Region A surrounding the earth near the equator is the area where the magnetic field is depressed by the ring current.

Values of ΔB change with magnetic activity in different ways in different regions. Contour maps for ΔB for the noon-midnight and dawn-dusk meridian planes for slightly disturbed periods of Kp = 2-3 have been drawn, but are not shown in this paper. These contours show an enhancement of the ring current intensity, particularly in the midnight meridian, and increases in +ΔB in Region B, including the polar cap magnetosphere. Magnitudes of -ΔB in Region C on the day side increase, and Region C expands so that this region becomes connected to the equatorial Region A. Thus in some areas, even at low latitudes, the field reduction from the magnetopause current is superimposed on that from the ring current. Need for caution in interpreting observational results in such areas is clearly indicated. This point will be discussed later in connection with magnetic storms. The minimum ΔB in Region A is in the vicinity of 3 R_e in all half-planes for midnight, dawn, noon and dusk.

From the ΔB contour map for Kp = 0-1 shown in Figure 1 and that for Kp = 2-3 (not shown) it is clear that the equatorial region of field depressions (Region A) extends roughly from 10 R_e to $\leq$ 3 R_e near midnight at magnetically quiet times and during weakly disturbed periods. Under these magnetic conditions, therefore, the ring current distribution is continuous from the tail current. It is probably more appropriate to say that the tail current extends earthwards to the inner boundary of the plasma sheet, i.e. to the plasmapause, and that the current distribution further continues inward into the plasmasphere with its maximum intensity in the vicinity of 3 R_e, or possibly at a closer distance from the earth at times. This view is in strong contrast to the usual concept of the quiet-time ring current which is a toroidal current belt situated at about 6.5 R_e (e.g., Frank, 1971).

There are two questions that must be carefully examined to establish that the above $-\Delta B$ distribution at close distances to the earth is real. These concern (a) the accuracies of the satellite orbits and (b) the accuracies in the reference fields used to derive ΔB from the OGO 3 and 5 data. Regarding the question (a), there are several reasons to believe that the orbit accuracies are adequate for our present discussion at geocentric distances ≥ 2.5 R_e and very likely even at 2 R_e. On many orbits of both OGO's 3 and 5 the satellite crossing of the dipole equator took place near perigee. On these occasions the ΔB minimum, i.e. the maximum absolute value of ΔB, was observed consistently near the dipole equator crossing rather than at perigee. An example of this circumstance is shown in Figure 3. The orbit characteristics of the two satellites changed greatly during the several years of operation. The inclinations of the satellites which were initially 31° at launch increased gradually; for instance, OGO 3 became a near polar orbiting satellite when the Rb magnetometer experiment was re-activated for one year from February 1971 to February 1972. Nevertheless the ΔB data from both OGO's 3 and 5 continued to show the same orderliness when arranged according to dipole coordinates. Systematic errors in orbit information are highly unlikely to be ordered by dipole coordinates and also to result in geomagnetic time variations. Another argument given below using a quantity $\Delta(\Delta B)$ is also a strong reason to believe that the orbit errors are insignificant in the present discussion.

The question (b) concerns whether or not the large negative values of ΔB at close distances, say < 4 R_e, are due to errors in the reference fields on which the calculations of ΔB were based. The latest internal field model existing at the time the orbit calculation scheme was made prior to launch was used in the analysis in each case of OGO's 3 and 5, because the reference field data were available on orbit tapes. Thus the reference fields were based on two different models (Sugiura et al., 1971, for details). However, differences between the two models are insignificant in our present discussion. A detailed comparison of various models has shown that it would not have made any significant difference in the present results even if the most recent reference field was used. The averaging over longitudes to derive the (dipole) local time dependence, in any case, tends to smooth out the differences between different models. The possibility that all the reference fields are in error so as to create large $-\Delta B$ values near the dipole equator has been carefully examined. This possibility can be almost, if not completely, ruled out by examining the r-dependence of ΔB, for instance, by comparing ΔB at 4 R_e and at 2 R_e when various terms in the spherical harmonic expansion are slightly changed. Generally, if a reasonable size of ΔB is artifically created at 4 R_e by changes in the expansion, the resulting $|\Delta B|$ at 2 R_e becomes too large. Ness (1971) reached a similar conclusion, i.e. that the use of a slightly different dipole coefficient for the reference field will not significantly alter the location of observed magnitude anomaly.

The strongest argument that the observed large negative ΔB values at ~ 3 R_e are real can be presented by taking differences between ΔB for Kp = 2-3 and ΔB for Kp = 0-1 at a network of points in a meridian plane and thereby expressing the differences in ΔB as a function of radial distance and dipole latitude. By so doing the question of the reference field and the possibility of systematic orbit errors can be completely eliminated. Contours for such differences, which may be called $\Delta(\Delta B)$, for the midnight meridian are shown in Figure 4. The quantity plotted can be thought of as the derivative of $\Delta B(Kp)$ with respect to Kp, evaluated at Kp = 1.5. The general characteristics of the contours are remarkably similar to those for ΔB itself in both $-\Delta B$ and $+\Delta B$ regions. With this figure the reality of the $-\Delta B$ distribution at close distances, at least to 2 R_e, can be considered as being established. The $\Delta(\Delta B)$ distribution, on which Figure 4 is based, shows that $\Delta(\Delta B)$ is almost uniform over the large area from about 2 to 8 or 9 R_e near midnight. This means that the ring current was intensified nearly at all distances from 2 or 3 R_e to at least 11 R_e. That the $\Delta(\Delta B)$ distribution of this type cannot be produced by a toroidal ring current will become clear in later discussions. In the noon meridian the average $\Delta(\Delta B)$ distribution is found to be more irregular than for midnight and the only distinct feature to be noted is that $\Delta(\Delta B)$ is approximately -10γ between 2 and 3 R_e and within 15° of the dipole equator. It is of interest to note that the integrated magnetic flux decrease between 2 and 3 R_e within a small dipole local time increment,

$\Delta\phi$, at noon is almost 1/20 of the integrated flux decrease within $\Delta\phi$ at midnight between 2 and 11 R_e. However, the most significant feature is that the intensified ring current extends to well inside the plasmapause.

Re-examination of Earlier Observations

In the new light of the ΔB topology determined from the OGO 3 and 5 observations most of the earlier results discussed in the literature are found to fall into proper place in nearly every aspect. There have been misinterpretations in the absence of the knowledge of the ΔB distribution to be used as a reference, but some of the speculative interpretations are, interestingly enough, found to be not too far off from the reality. Figure 5 shows the scalar field measurements obtained by Explorer 10 at 2 to 7 R_e (Heppner et al., 1963). The reference field was based on the then available set of spherical harmonic coefficients by Finch and Leaton. The resultant ΔB shows both $-\Delta B$ up to ~ 4 R_e and $+\Delta B$ at larger distances. Heppner et al. attempted to correct the Finch-Leaton reference field by applying a correction based on the Vanguard 3 measurements. Using the corrected reference field, they noted that the maximum percentage difference in the field was at 2.5 R_e. They remarked that the existence of a quiet-day diamagnetic ring current with maximum intensity located lower than the 3 R_e magnetic shell along the Explorer 10 trajectory (or roughly 3.8 R_e at the equator) is possible. Though the accuracies of the orbit and the reference field may be questionable, the Explorer 10 results are interesting in that observations of $-\Delta B$ and $+\Delta B$ were made in appropriate regions when viewed with reference to the new ΔB distribution.

The observations on Luniks 1 and 2 showed very large negative ΔB in the inner magnetosphere, but these ΔB values were too large in magnitudes to be real. Electron 2 observed a field depression at $5 \sim 7$ R_e and extending inward with increasing magnitude to ~ 3 R_e in the nightside magnetosphere (Dolginov et al., 1966). These observations indicated a minimum ΔB values of -100 to -150γ at 3 R_e on normal days. Inaccuracies in the orbit and the reference field used probably caused the large ΔB magnitudes, but their observations seem to be qualitatively in gross agreement with the present results for both $-\Delta B$ and $+\Delta B$. It is interesting to note that Yeroshenko (1966) and Dolginov et al. (1966) observed increases in $+\Delta B$ during magnetically disturbed periods; they were seeing variations in the $+\Delta B$ region in terms of the present ΔB topology.

Figure 6 gives an example of Explorer 12 observations on a quiet day (on the morning side of the magnetosphere) obtained by Cahill and Bailey (1967) which can now be interpreted as showing a traversal of the satellite from the $-\Delta B$ region to the $+\Delta B$ region. Cahill and Bailey remarked that the measured field appears to be slightly lower than predicted from L = 5-7 but not significantly so in view of the estimated accuracy of the data. Such transitions from the $-\Delta B$ to $+\Delta B$ regions or vice versa are evident in many examples shown by Cahill and his associates. They interpreted $+\Delta B$ as being the effect of the ring current. However, $+\Delta B$ could be partially or mostly from other sources depending upon the latitude and local time of the position.

Toroidal Ring Current Models

The theoretical models presented by Akasofu and Chapman (1961), Apel et al. (1962), Akasofu et al. (1962), and Hoffman and Bracken (1965, 1967) assume a toroidal belt of ring current particles. It is important to see that this type of ring current when applied to the average quiet-time condition does not fit the observation. A comparison between the Hoffman-Bracken model of the quiet-time ring current and the OGO 3 and 5 observations is shown in Figure 7 in terms of ΔB on the dipole equator. The ΔB curve for the model has a deep minimum near the core of the toroidal ring current belt and recovers substantially on the earthward side before leveling off toward the earth, while the observed ΔB continuously decreases with decreasing distance to ≤ 4 R_e. Another notable difference between the model and the observations is seen for midnight; the observed ΔB does not become positive till well beyond 10 R_e at midnight, while the model predicts large $+\Delta B$ values outside the toroidal belt. The substantial recovery of $-\Delta B$ on the earthward side of the ring current belt stems

from the steep gradient in the particle pressure in the inner boundary of the particle belt. To support the particle pressure the current, $\underline{j}$, is eastward so that the $\underline{j} \times \underline{B}$ force balances the pressure gradient. Steep ΔB changes predicted by the theoretical models have not been observed at least at geocentric distances greater than about 1.6 R_e.

We have made extensive model calculations in an attempt to reduce the large discrepancy between the model and the observations at midnight. Figure 8 shows an example, in which the equatorial ΔB is given using the Mead model for the magnetopause current and the Mead-Williams model for the tail field; an axially symmetric ring current distributed over the geocentric distances from 2.5 to 6.5 R_e as shown at the bottom of the figure is superimposed on the remaining components of the model field. Even with this relatively broad ring current the ridge in ΔB at midnight beyond the location of the ring current is too conspicuously different from the observation. By attempting to eliminate such a discrepancy a conclusion has been reached that the quiet-time ring current is continuous from the inner magnetosphere to the neutral sheet current in the tail. It is more appropriate to say that the tail current extends to inner regions of the magnetosphere. Indeed, to my knowledge no observational evidence seems to exist that indicates that the tail current, or the neutral sheet current, abruptly terminates at some distance. At best we know very little about the current distribution in the near earth tail region. However, the tail current estimated from $\nabla \times \underline{B}$ by Speiser and Ness (1967) based on the IMP 1 observations does indicate a circular current pattern around the earth at least beyond geocentric distance of 10 R_e near the dawn meridian as seen in Figure 9.

A remark is made here regarding the inner edge of the ring current where ΔB recovers rather steeply because of the eastward current. Examining the Electron 2 results of Eroshenko et al. (1965), Heppner (1967) noted frequent observations of a rather abrupt change in slope of ΔB (in the direction of increased magnitude) near 3 R_e which resembled the feature observed by Explorer 10. He also noted that in both Electron 2 and Explorer 10 results there was not any obvious tendency for the ΔB deviation to turn back toward zero at 3 R_e. Thus he implied that the location of the lower limit of the ring current is less than 3 R_e. However, these discussions should be taken with certain reservation because of the uncertainties arising from the orbit accuracies and the reference fields, and in some cases, from the consequence of the fluxgates being near saturation, and poor resolutions coming from digitization steps. Nevertheless, these early observations share a common ground with the recent OGO 3 and 5 observations for locating the inner boundary of the ring current at distances < 3 R_e. For the lower limit to the position of the ring current the Vanguard 3 observations put this to be above 1.4 R_e on the equator (Heppner et al., 1961, Cain et al., 1962).

In their analysis of magnetic storm data from ATS 1 Coleman and Cummings (1971) became aware of the difficulty in separating the ring current and tail current effects at the synchronous orbit. They suggested that during the early phase of the main phase the ring current and neutral sheet plasmas are contiguous, at least intermittently, and that they become separated during the recovery phase. Although a unique interpretation is not possible from observations at the synchronous orbit alone, their speculation is partially in agreement with the view presented here. A serious disagreement, however, is that the continuity of the current from the tail to the ring current as deduced in this paper is a condition that prevails even at quiet times.

Ring current Particles

The first detection of particles that were thought to be responsible for the ring current was made by Davis and Williamson (1963) on Explorer 12. They observed a large flux of trapped protons in the energy range 100 kev to 4.5 Mev with peak intensity at L = 3.5. Using preliminary Explorer 12 data, Akasofu et al. (1962) presented a model for the quiet-time ring current which causes an equatorial field depression of -38γ at the earth's surface and a maximum field reduction of -72γ

at 4.1 R_e. Hoffman and Bracken (1965) have since produced a model with a more thorough analysis of the Explorer 12 results; in their model, ΔB, on the equator is -11γ at the earth's surface and is a minimum at L = 3.6 with ΔB of -23γ. As has already been discussed these theoretical models do not agree with the recent OGO 3 and 5 results in several important points.

The Explorer 12 observations of protons (> 100 kev) were confirmed by subsequent measurements by Explorers 14 and 15 (Davis, 1965). Hoffman and Bracken (1967) extended their study of the quiet-time ring current and constructed a storm-time ring current model in which the magnetic field and the particle distribution are made self-consistent by successive approximations in a similar manner but with considerable improvements to the earlier studies by Beard (1962) and Akasofu et al. (1961). Referring to the quiet-time ring current, Hoffman and Bracken (1965) noted that the lifetime of the protons considered to be responsible for the quiet-time ring current is relatively short, being of the order of a week (Liemohn, 1961), and thus that to sustain a quiet-time belt the particles must be continuously replenished. On the other hand such a lifetime is considerably longer than the initial, fast decay time for the main phase of a magnetic storm discussed by Akasofu (1963).

Frank (1967, 1968, 1970, 1971) has made comprehensive observations of low energy protons in the energy range from 200 ev to 50 kev on OGO 3. In particular, for the moderate magnetic storm of early July 1966 he showed proton intensity profiles as functions of L for pre-storm, main phase, recovery, and post-storm conditions, which clearly indicate the development and decay of the ring current (Frank, 1967). During the main phase the maximum intensity for protons with energy 31 to 49 kev was observed at L = 3.6 in gross agreement with the position of the center of the ring current as inferred by Cahill (1966) from the magnetic field measurements made during another magnetic storm. Using the relation between the field depression at the equator on the earth's surface and the total energy of the particles contributing to the ring current, derived by Dessler and Parker (1959) and Scopke (1966), Frank (1967) showed that the total energy of the observed protons (200 ev $\lesssim$ E $\lesssim$ 50 kev) is adequate to produce the field reduction on the ground as indicated by Dst. He estimated that electrons in the same energy range contributed about 20% of the ring current. Electron flux increases during storms or magnetically active periods had been observed by Explorer 12 (Freeman, 1964; Frank, 1966).

Frank (1967) also presented evidence for the development of a partial ring current during the main phase of two storms in July and September 1966. He showed, in his Figure 1, proton (31 $\le$ E $\le$ 49 kev) directional intensities as functions of L during several phases of the storms. However, it is noted that the satellite was near the dipole equator along the inbound pass and was at higher latitudes on the outbound pass. Although the existence of a partial ring current belt cannot be questioned in most storms, it is difficult to assess to what extent the comparisons between the inbound and outbound passes of OGO 3 represent true axial asymmetry without knowing latitude effects. From the standpoint of the ΔB topology the inbound passes penetrate through the core of the $-\Delta B$ region but the outbound orbits partially lie in the peripheral areas of the $-\Delta B$ region and partially in the $+\Delta B$ region. However, his inbound observations must represent very nearly the true dependence of the proton intensity in the above energy range on the radial distance on the dipole equator from L of 8 to 4 R_e; below L of 4, the sharp decrease of the proton intensity may partially be due to latitude effects.

We now turn to the problem of the quiet-time ring current. Frank (1971) has studied the complex structure of the near-earth termination of the plasma sheet near midnight. He presented several examples of energy density profile for low energy protons (90 ev $\le$ E $\le$ 48 kev) and electrons (80 ev $\le$ E $\le$ 46 kev) as functions of L near local midnight obtained on OGO 3. Using the magnetic field measurements on the same satellite, plasma parameter β, defined as the ratio of the plasma energy density to the magnetic field energy density, can be calculated. Figure 10 shows an example of plots of β, the scalar field B, and the difference field ΔB. Values of β are near unity in the vicinity of the peak plasma energy density, i.e. at about 6.5 R_e.

Recognizable field reductions are found near this high β region. However, the large field depressions well inside the plasmasphere at 4 to 3 R_e cannot be caused by the high β plasma near 6.5 R_e. Similar features are observed on all six orbits of OGO 3 for which Frank (1971) published plasma energy density profiles. Thus it is concluded that the proton belt near 6.5 R_e which Frank called the "extraterrestrial ring current" in magnetic quiescence is only a part of the quiet-time ring current and that the main source of the core of the quiet-time ring current inside the plasmasphere escaped detection by Frank's experiment.

What then causes the large field reduction inside the plasmasphere? A promising answer seems to have come quite recently from the Explorer 45 (S^3) observations of protons with energy from 5 to 872 kev by Smith and Hoffman (1972). In their study of the magnetic storm of December 16-18, 1971, they obtained proton energy density profiles for a pre-storm period and several storm phases. In the profile taken before the sudden commencement the maximum energy density of approximately 2×10^{-7} ergs cm^{-3} was observed at about L = 3.5. Between L of 2.5 and 4 the main contribution to the total energy density came from the protons with energies from 362 to 872 kev. Equating this energy density to the field distortion energy density $B\Delta B/4\pi$, ΔB is -35γ at 3.5 R_e on the dipole equator. This is a crude order-of-magnitude estimate, but this ΔB value is nearly equal to the observed average ΔB at this distance. To establish that the principal contributer to the ring current in the plasmasphere is a population of protons having energies of 100 to several hundred kev, a more extensive study is required. During the main phase of the storm most of the energy density was carried by 12 to 100 kev protons, according to Smith and Hoffman. These protons must belong to the same population of protons that Frank had observed during storms.

One may question why the equatorial ring current protons in the plasmasphere had not been detected definitively by earlier observations by Davis on Explorers 12, 14, and 15. According to Davis (1965), there was a large region near the dipole equator between 1.4 and 4 R_e which was not covered by Explorer 12, and a similar situation existed with Explorer 14; he states that Explorer 15 filled the gap in this region of space. Retrospectively, Davis and Williamson (1963) and Davis (1965) seem to have observed protons of energies > 97 kev between L = 3 and 5 with sufficient energy densities to account for the quiet-time ring current at these distances. It is noteworthy that according to Davis (1965) the low energy proton intensities in the region L = 2 to 5 were constant within $\pm$ 25% during magnetically quiet periods in August and September of 1961 and October to December 1962.

With composite results from Explorers 12, 14, and 15 Davis (1965) estimated the total energy of protons having energy > 97 kev at 1.5×10^{22} ergs. This value is comparable with Frank's (1967) estimate of the total energy of protons with energy between 200 ev and 50 kev during slightly disturbed conditions; for a quiet day (June 23, 1966) the total energy estimate is 4.8×10^{21} ergs. Using the relation between the total energy, ϵ (in ergs), of the ring current particles and the field reduction ΔB (in γ) on the dipole equator at the earth's surface (Sckopke, 1966): $\Delta B = 2.6 \times 10^{-21}\ \epsilon$, Davis' estimate of the total proton energy (E > 97 kev) corresponds to ΔB of -39γ, which is approximately equal to the observed field decrease near the equator at 2 to 3 R_e. The current density distribution is sensitive to the particle pressure distribution as a function of radial distance. A study is being made if the low energy proton distribution which combines Davis' results and those obtained by Frank and Owens (1970) could account for the ΔB profile observed by OGO's 3 and 5.

A remark should be made on the question of whether or not the thermal plasma in the plasmasphere could contribute appreciably to the quiet-time ring current. According to Taylor et al. (1970) the H^+ density at 3 R_e is of order 1×10^3 ions cm^{-3}. The average ion temperature obtained by Serbu and Maier (1970) for the plasmasphere appears to be slightly higher on the dayside than on the dark side: the dayside average temperature is 3×10^4 °K near 3 R_e. These values for the density and temperature give the ion energy density, $\frac{3}{2}$ nkt, of 6×10^{-9} ergs cm^{-3}. If we assume, for simplicity, that the electrons have the same energy density, the total energy density

is 1.2 x 10^{-8} ergs cm^{-3}, or 7.5 kev cm^{-3}. This energy density is 1 order of magnitude less than is required for the observed field reduction near 3 R_e.

Rough energy density estimates, based on the charts of omnidirectional intensities for protons ($0.5 \leq E \leq 50$ kev) published by Frank and Owens (1970) show that outside the plasmapause, protons having energy 16 to 50 kev become the dominant source for the quiet-time ring current. The change in slope in ΔB observed near the plasmapause on some passes of both OGO's 3 and 5 may well represent the transition near the plasmapause in the main constituent of the ring current particles, namely from the population of protons ($100 \leq E \leq$ several hundred kev) inside the plasmasphere to another population of protons ($10 \leq E \leq 50$ kev) in the plasma sheet. The ΔB variation shown in Figure 10 is a good example indicating this possibility. However, there are many passes on which ΔB decreases monotonically with decreasing radial distance without any distinct transition in the vicinity of the plasmapause. It may be that on these passes the plasma pressure was nearly constant or its gradient was small in the vicinity of the plasmapause. It should be noted here, however, that the spatial variations in ΔB must be interpreted with proper care regarding the changes in both radial distance and dipole latitude.

Summary and Conclusions

The topology of the scalar difference field ΔB based on the OGO 3 and 5 observations was presented. This ΔB distribution provided a scheme according to which the complex features of ΔB found in various regions of the magnetosphere by the earlier magnetic field measurements on numerous U.S. and Russian satellites and space probes can be clearly sorted out and properly interpreted.

The reality of the large field depressions in the equatorial region deep inside the plasmasphere extending earthward at least to 2 R_e is now well established. This field depression is on the average about 40γ on the dipole equator at geocentric distance of 3 R_e under magnetically quiet conditions with Kp = 0-1. Protons having energy 100 to several hundred kev, first observed by Davis and Williamson (1963) on Explorer 12 and very recently by Smith and Hoffman (1972) on Explorer 45, must be responsible for the inner ring current; the energy density of these protons is comparable to the magnetic field energy density associated with the field distortion of the observed magnitude. The intensity of the inner ring current varies with magnetic activity as represented by Kp, even for relatively low activity level of Kp = 2 or 3.

It has been argued that the equatorial tail current extends earthward to the plasmapause or a little beyond the plasmapause and continues on to the inner ring current. The extension of the tail current, which may be called the outer ring current, is carried mostly by protons of energy near 50 kev and below, observed by Frank (1967, 1971). Thus the outer ring current is essentially the current in the plasma sheet. At least part of the outer ring current encircles the earth and flows in the dayside magnetosphere.

The interpretation that the inner ring current is an extension of the tail current in the plasma sheet has a very important implication in that the plasma pressure near the dipole equator is approximately constant or varies only gradually with geocentric distance without any discontinuity in the vicinity of the plasmapause. Since the thermal plasma pressure is approximately 1 order of magnitude less than the pressure of the 'ring current plasma', the pressure balance at the plasmapause is readily achieved by a slight adjustment in the ring current plasma pressure across the plasmapause. When the plasma sheet moves inward during a magnetospheric substorm, the increase in the pressure in the plasma sheet is conveyed directly to the ring current particles inside the plasmasphere, thereby enhancing the current intensity in the inner ring current. In this picture there does not seem to be any difficulty for the 10 to 50 kev protons in the plasma sheet to penetrate into the inner ring current region and become the dominant source of current during a magnetic storm.

Though the gross features of the field distortion (or inflation) by the ring

current and of the particles responsible for the ring current appear to have been clarified, details of the development and decay of the ring current during substorms, magnetic storms, and other less pronounced disturbances must be studied in the future. It has been shown in this paper that dipole latitude is an important parameter in analyses of particle and magnetic field measurements relative to the ring current. The problem of the +ΔB region at mid to high latitudes on the dark side of the magnetosphere and extending sunward on both sides of the earth beyond the dawn and dusk meridian half-planes is partially related to the inflation of the equatorial magnetosphere, but is more fundamentally related to the solar wind-magnetosphere interaction on the magnetopause, and as such it is outside the scope of this paper. However, this problem must be kept in mind in interpreting magnetic field observations in the magnetosphere.

References

Akasofu, S.-I., Space Sci. Rev., 2, 91, 1963.

Akasofu, S.-I., Space Sci. Rev., 6, 21, 1966.

Akasofu, S.-I., and S. Chapman, J. Geophys. Res., 66, 1321, 1961.

Akasofu, S.-I., and S. Chapman, Planet. Space Sci., 12, 607, 1964.

Akasofu, S.-I., J. C. Cain, and S. Chapman, J. Geophys. Res., 66, 4013, 1961.

Akasofu, S.-I., J. C. Cain, and S. Chapman, J. Geophys. Res., 67, 2645, 1962.

Apel, J. R., S. F. Singer, and R. C. Wentworth, Advances in Geophysics, Vol. 9 pp. 131-189, Academic Press, New York, 1962.

Beard, D. B., J. Geophys. Res., 67, 3615, 1962.

Cahill, L. J., Jr., J. Geophys. Res., 71, 4505, 1966.

Cahill, L. J., Jr., (Abstract), Am. Geophys. Union, 53rd Annual Meeting, Washington, D. C., 1972.

Cahill, L. J., Jr., and D. H. Bailey, J. Geophys. Res., 72, 159, 1967.

Cain, J. C., I. R. Shapiro, J. D. Stolarik, and J. P. Heppner, J. Geophys. Res., 67, 5055, 1962.

Chapman, S., Geophysics, The Earth's Environment, pp. 373-502, Gordon and Breach, Science Publishers, New York, 1963.

Coleman, P. J., Jr., and W. D. Cummings, Radio Sci., 3, 762, 1968.

Coleman, P. J., Jr., and W. D. Cummings, J. Geophys. Res., 76, 51, 1971.

Cummings, J., J. Geophys. Res., 71, 4495, 1966.

Davis, L. R., Proc. Plasma Space Science Symposium, edited by C. C. Chang and S. S. Huang, pp. 212-226, D. Reidel Publishing Company, Dordrecht-Holland, 1965.

Davis, L. R., and J. M. Williamson, Space Res., 3, 365, 1963.

Dessler, A. J., and E. N. Parker, J. Geophys. Res., 64, 2239, 1959.

Dolginov, Sh. Sh., Ye. G. Yeroshenko, and L. N. Zhuzgov, Space Res., 6, 790, 1966.

Eroshenko, E. G., Sh. Sh. Dolginov, L. N. Zhuzgov, U. V. Fastovsky, and L. M. Alexanyan, Space Res., 5, 980, 1965.

Fejer, J. A., Can. J. Phys., 39, 1409, 1961.

Frank, L. A., J. Geophys. Res., 71, 4631, 1966.

Frank, L. A., J. Geophys. Res., 72, 3753, 1967.

Frank, L. A., J. Geophys. Res., Physics of the Magnetosphere, edited by R. L. Carovillans, J. F. McClay and H. R. Radoski, pp. 271-289, 1968.

Frank, L. A., J. Geophys. Res., 75, 1263, 1970.

Frank, L. A., J. Geophys. Res., 76, 2265, 1971.

Frank, L. A., and H. D. Owens, J. Geophys. Res., 75, 1269, 1970.

Freeman, J. W., Jr., J. Geophys. Res., 69, 1691, 1964.

Heppner, J. P., Physics of Geomagnetic Phenomena, edited by S. Matsushita and W. H. Campbell, Vol. 2, pp. 935-1036, 1967.

Heppner, J. P., J. C. Cain, I. R. Shapiro, and J. D. Stolarik, NASA TN D-696, 1961.

Heppner, J. P., N. F. Ness, C. S. Scearce and T. L. Skillman, J. Geophys. Res., 68, 1, 1963.

Hoffman, R. A., and P. A. Bracken, J. Geophys. Res., 70, 3541, 1965.

Hoffman, R. A., and P. A. Bracken, J. Geophys. Res., 72, 6039, 1967.

Liemohn, H., J. Geophys. Res., 66, 3593, 1961.

Ness, N. F., Goddard Space Flight Center Report X-690-71-465, 1971.
Parker, E. N., J. Geophys. Res., 71, 4485, 1966.
Scopke, N., J. Geophys. Res., 71, 3125, 1966.
Serbu, G. P., and E. J. R. Maier, J. Geophys. Res., 75, 6102, 1970.
Smith, P. H., and R. A. Hoffman, (Abstract), Am. Geophys. Union 53rd Annual Meeting, Washington, D. C., 1972.
Speiser, T. W., and N. F. Ness, J. Geophys. Res., 72, 131, 1967.
Sugiura, M., B. G. Ledley, T. L. Skillman, and J. P. Heppner, J. Geophys. Res., 76, 7552, 1971.
Taylor, H. A., H. C. Brinton, and A. R. Deshmukh, J. Geophys. Res., 75, 2481, 1970.
Yeroshenko, Ye. G., Space Res., 6, 629, 1966.

Figure Captions

Figure 1: ΔB contours in the noon-midnight meridian plane for magnetically quiet periods, Kp = 0-1.

Figure 2: ΔB contours in the dawn-dusk meridian plane for magnetically q periods, Kp = 0-1.

Figure 3: ΔB observed by OGO 5 near perigee.

Figure 4: $\Delta(\Delta B)$ in the midnight meridian plane defined as the difference between ΔB for Kp = 2-3 and ΔB for Kp = 0-1. ΔB values in the northern and southern hemispheres are averaged.

Figure 5: Explorer 10 magnetic field observations at geocentric distances 2 - 7 R_e (from Heppner et al., 1963).

Figure 6: An example of Explorer 12 observations on a quiet day (from Cahill and Bailey, 1967). ΔB is indicated by vertical lines drawn from the projection of the orbit. End of lines, dotted, is above the orbit curve for $\Delta B > 0$ and below it for $\Delta B < 0$.

Figure 7: Comparison of the equatorial ΔB computed using the Hoffman-Bracken model and the observed average ΔB at noon and midnight (from Sugiura et al., 1971).

Figure 8: Equatorial ΔB with a ring current with an intensity distribution shown in the bottom.

Figure 9: The tail current distribution computed from curl $\underline{B}$ (from Speiser and Ness, 1967).

Figure 10: Plasma parameter β, the scalar field intensity B, and the difference scalar field intensity ΔB, measured on OGO 3 near midnight.

EQUAL ΔB CONTOURS (OGO 3 & 5 Rb MAGNETOMETER OBSERVATIONS)

$\Delta B = B$ (MEASURED) $- B$ (REFERENCE FIELD)

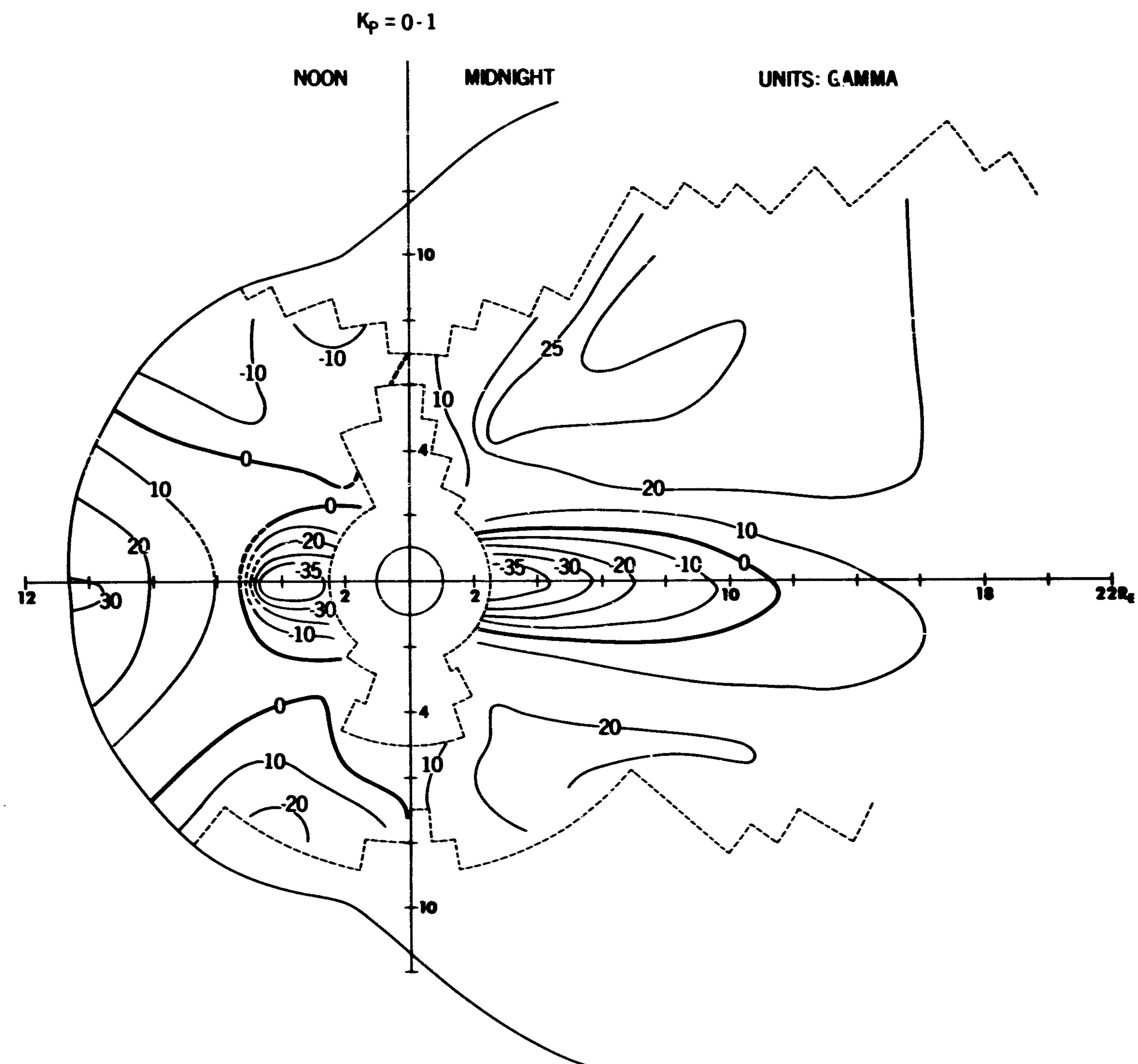

Figure I

EQUAL ΔB CONTOURS (OGO 3 & 5 Rb MAGNETOMETER OBSERVATIONS)
$\Delta B = B$ (MEASURED) - B(REFERENCE FIELD)

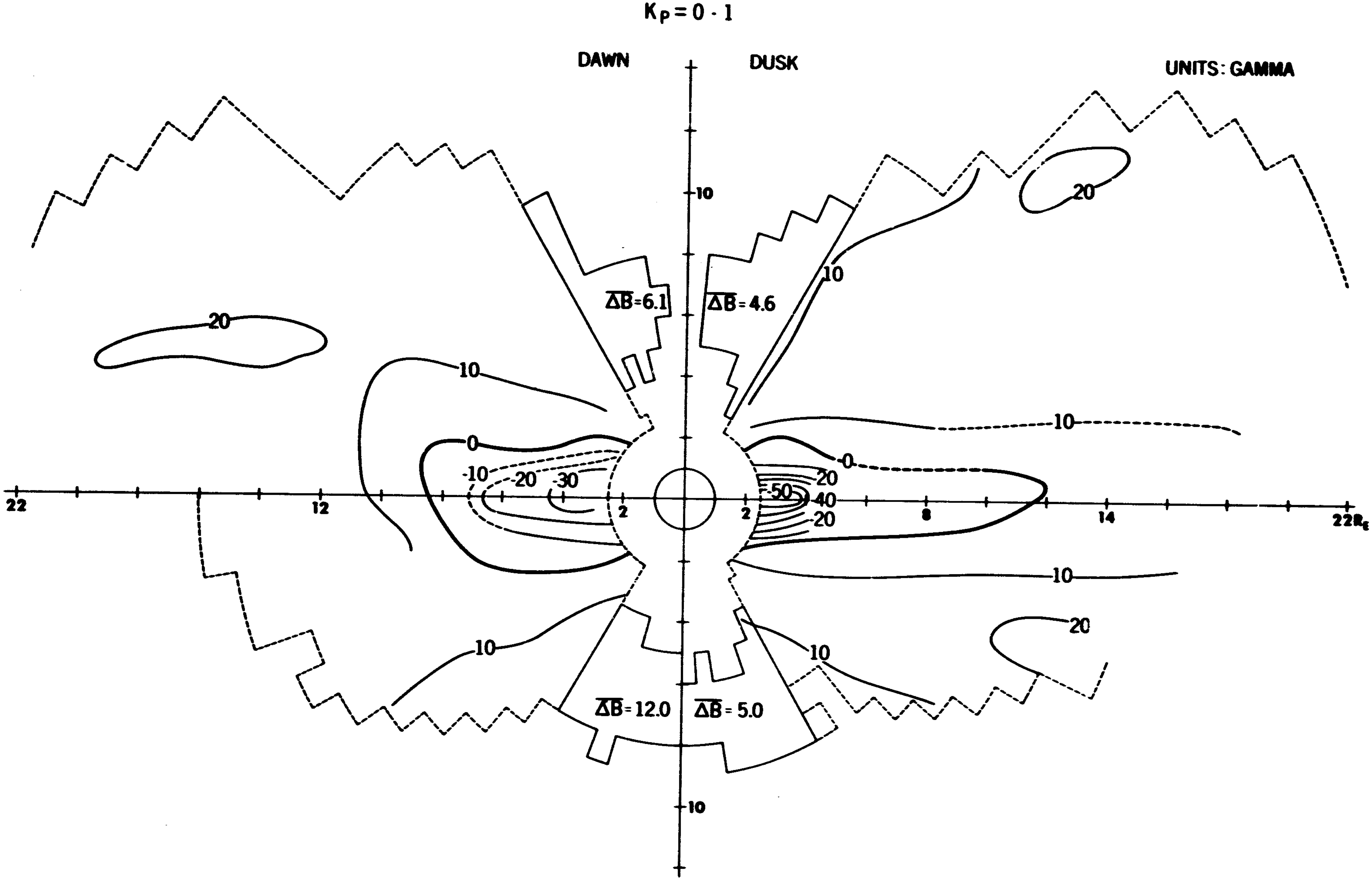

Figure 2

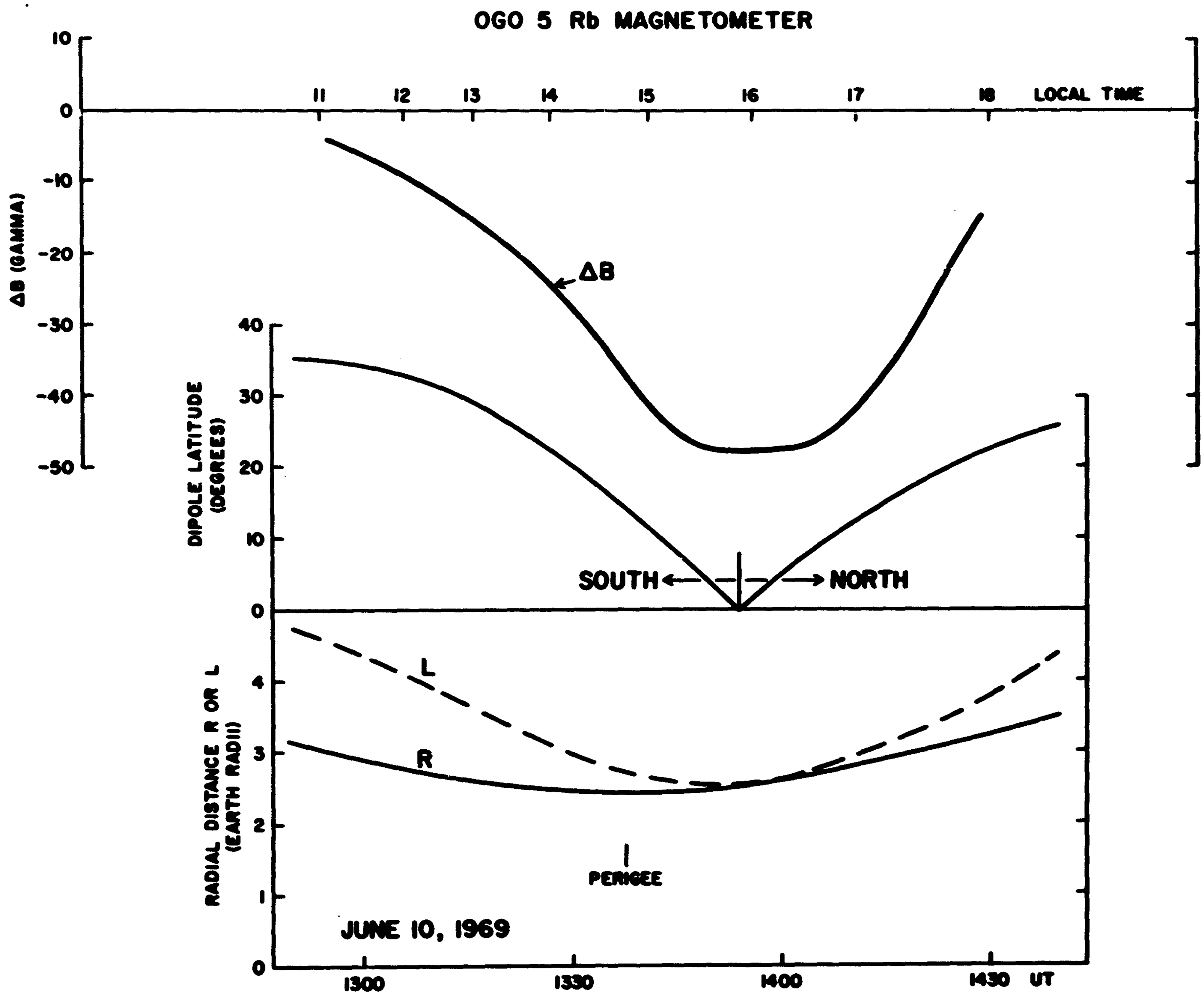
OGO 5 Rb MAGNETOMETER
ΔB (GAMMA)
10
0
-10
-20
-30
-40
-50
11
12
13
14
15
16
17
18
LOCAL TIME
ΔB
DIPOLE LATITUDE (DEGREES)
40
30
20
10
0
SOUTH
NORTH
RADIAL DISTANCE R OR L (EARTH RADII)
4
3
2
1
0
L
R
PERIGEE
JUNE 10, 1969
1300
1330
1400
1430
UT

Figure 3

CONTOURS FOR $\Delta B(K_p=2\text{-}3)-\Delta B(K_p=0\text{-}1)$
MIDNIGHT QUADRANT

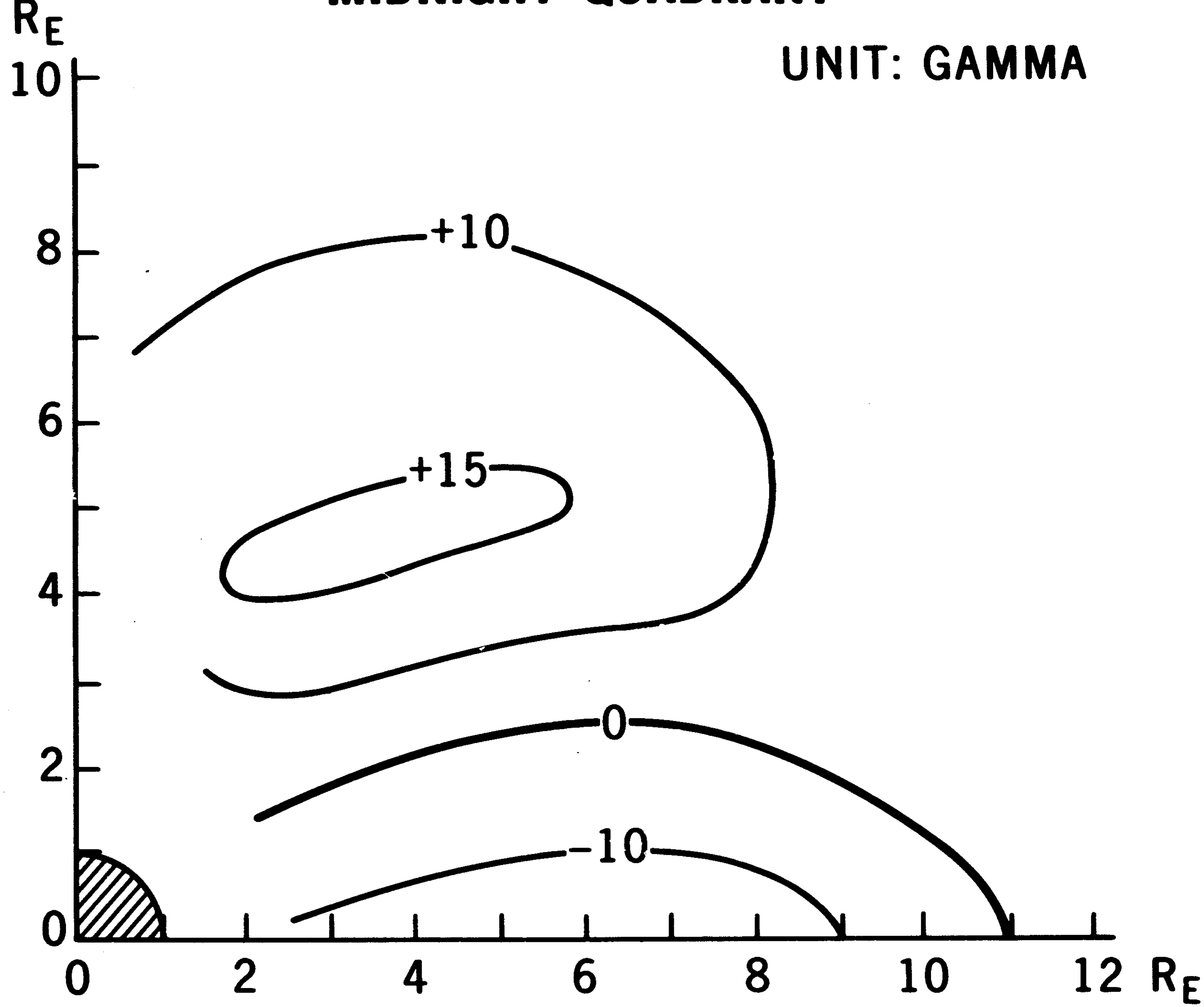

Figure 4

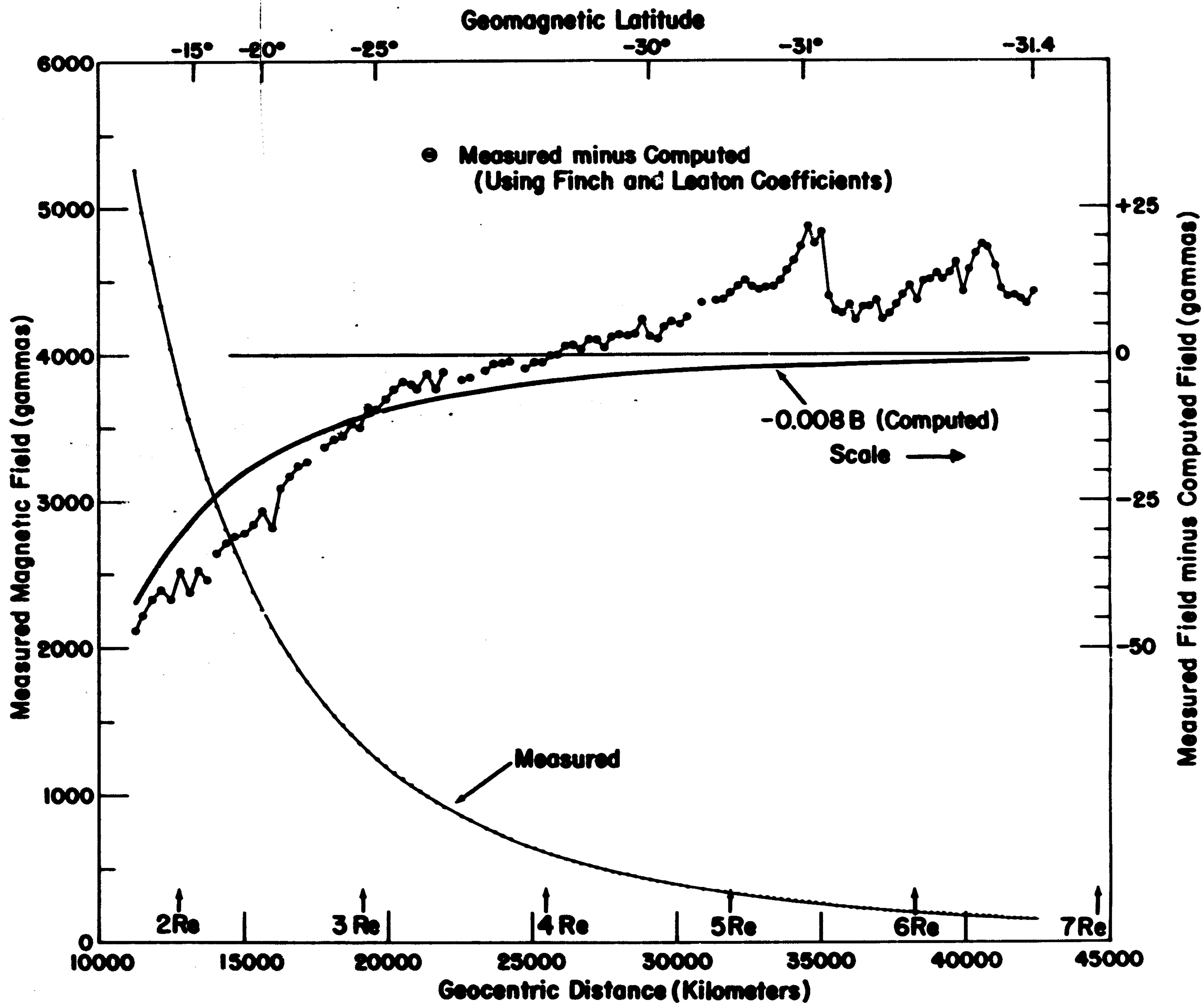

Geomagnetic Latitude
-15°
-20°
-25°
-30°
-31°
-31.4
Measured minus Computed
(Using Finch and Leaton Coefficients)
Measured Magnetic Field (gammas)
6000
5000
4000
3000
2000
1000
0
+25
0
-25
-50
Measured Field minus Computed Field (gammas)
-0.008 B (Computed)
Scale
Measured
2Re
3 Re
4 Re
5Re
6Re
7Re
10000
15000
20000
25000
30000
35000
40000
45000
Geocentric Distance (Kilometers)

Figure 5

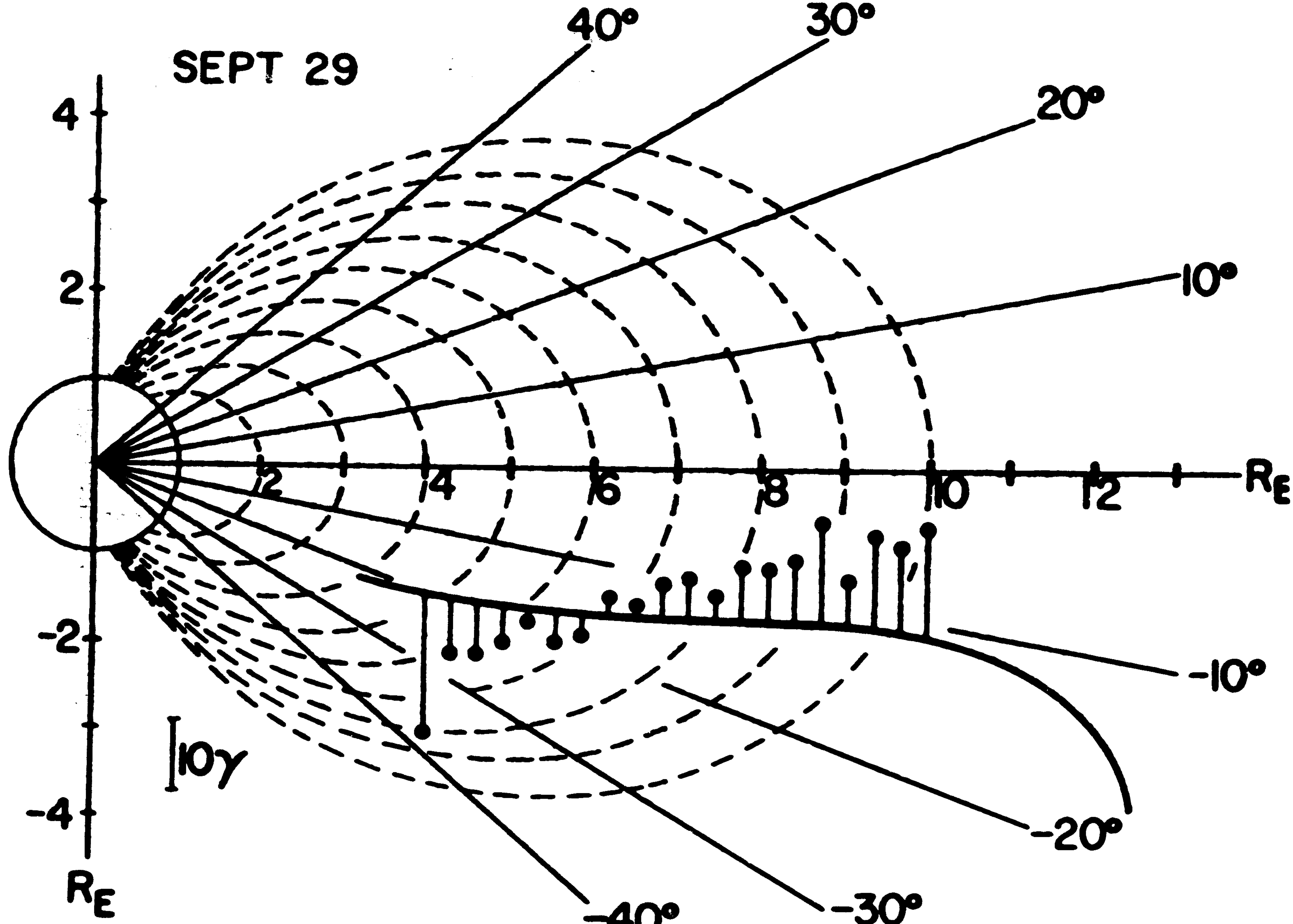

Figure 6

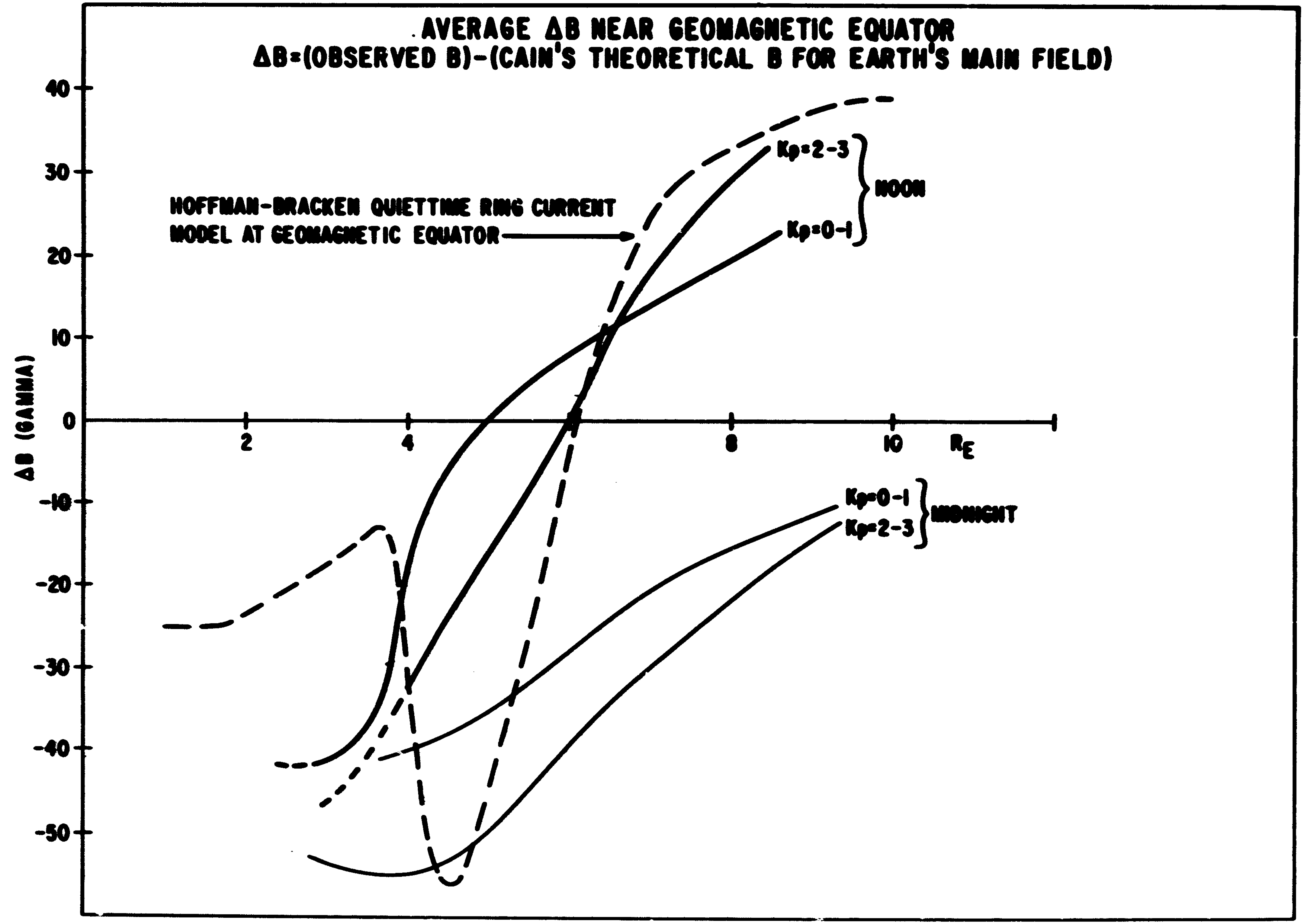
AVERAGE ΔB NEAR GEOMAGNETIC EQUATOR
ΔB=(OBSERVED B)-(CAIN'S THEORETICAL B FOR EARTH'S MAIN FIELD)
HOFFMAN-BRACKEN QUIETTIME RING CURRENT
MODEL AT GEOMAGNETIC EQUATOR
Kp=2-3
Kp=0-1
NOON
Kp=0-1
Kp=2-3
MIDNIGHT
ΔB (GAMMA)
40
30
20
10
0
-10
-20
-30
-40
-50
2
4
8
10
R_E

Figure 7

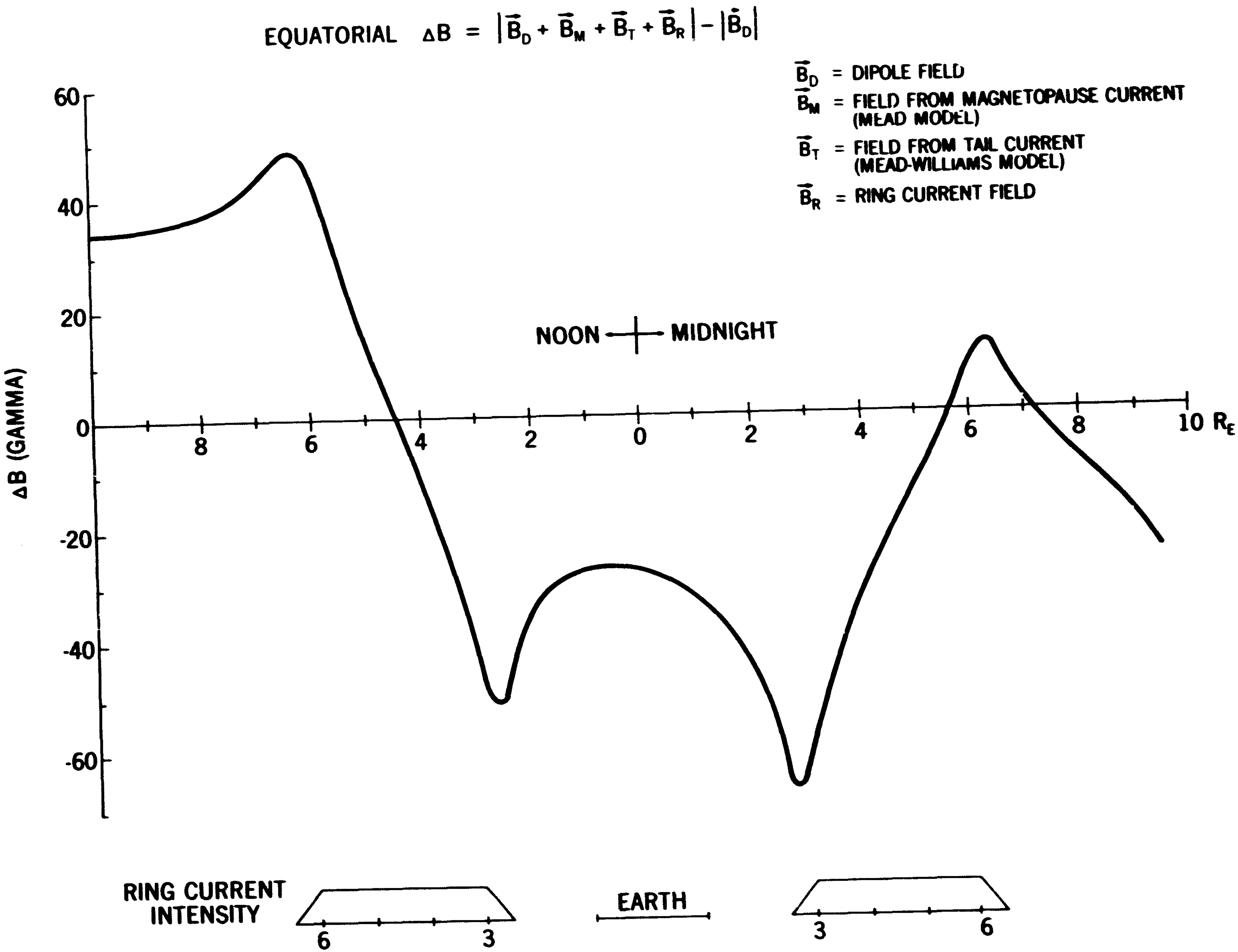
EQUATORIAL $\Delta B = |\vec{B}_D + \vec{B}_M + \vec{B}_T + \vec{B}_R| - |\vec{B}_D|$
$\vec{B}_D$ = DIPOLE FIELD
$\vec{B}_M$ = FIELD FROM MAGNETOPAUSE CURRENT (MEAD MODEL)
$\vec{B}_T$ = FIELD FROM TAIL CURRENT (MEAD-WILLIAMS MODEL)
$\vec{B}_R$ = RING CURRENT FIELD
NOON
MIDNIGHT
ΔB (GAMMA)
60
40
20
0
-20
-40
-60
8
6
4
2
0
2
4
6
8
10 R_E
RING CURRENT INTENSITY
6
3
EARTH
3
6

Figure 8

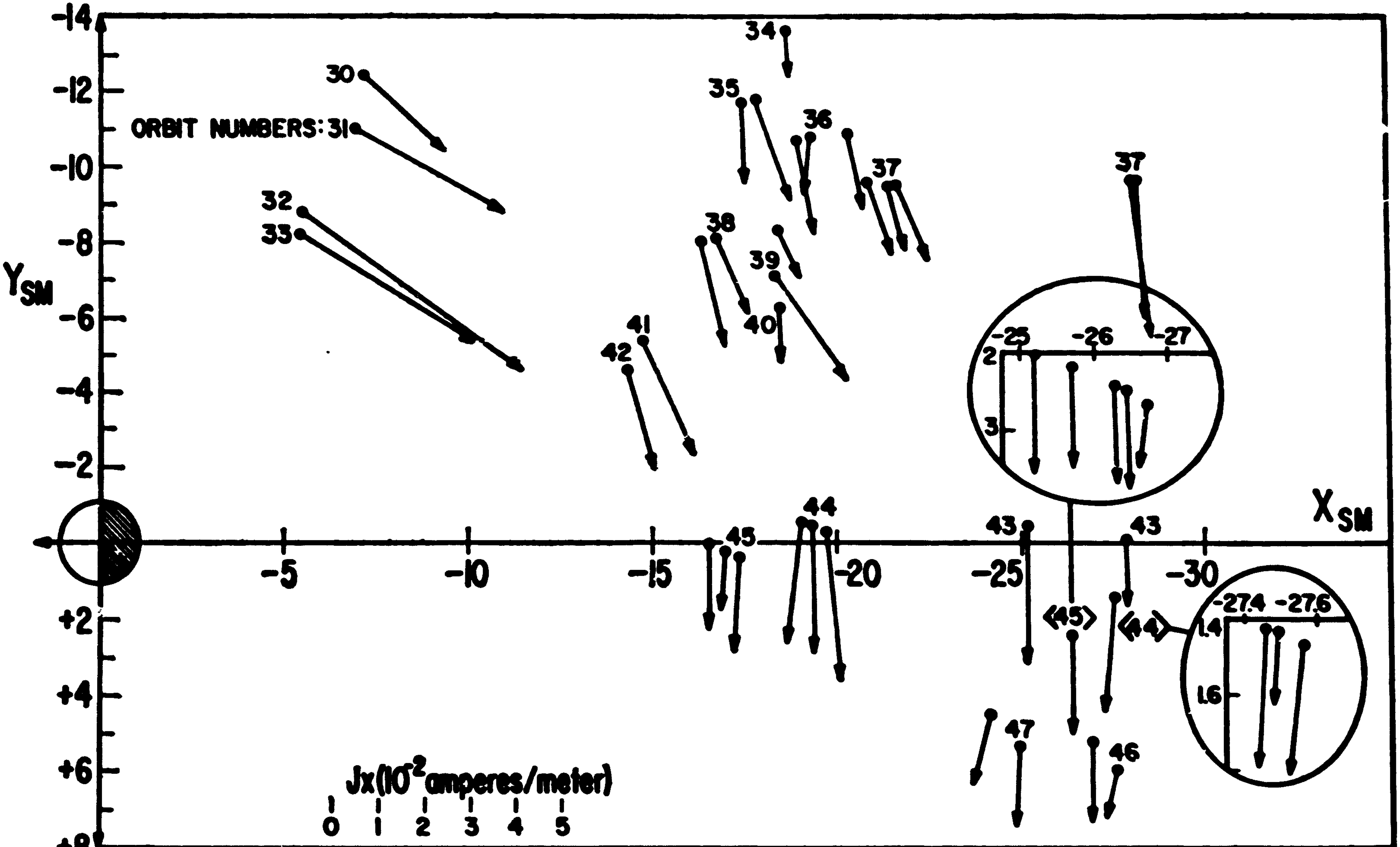
ORBIT NUMBERS: 31
30
32
33
34
35
36
37
38
39
40
41
42
43
44
45
46
47
⟨45⟩
⟨44⟩
Y_{SM}
X_{SM}
Jx(10^{-2} amperes/meter)
0 1 2 3 4 5
-14
-12
-10
-8
-6
-4
-2
+2
+4
+6
+8
-5
-10
-15
-20
-25
-30
-25 -26 -27
2
3
-27.4 -27.6
1.4
1.6

Figure 9

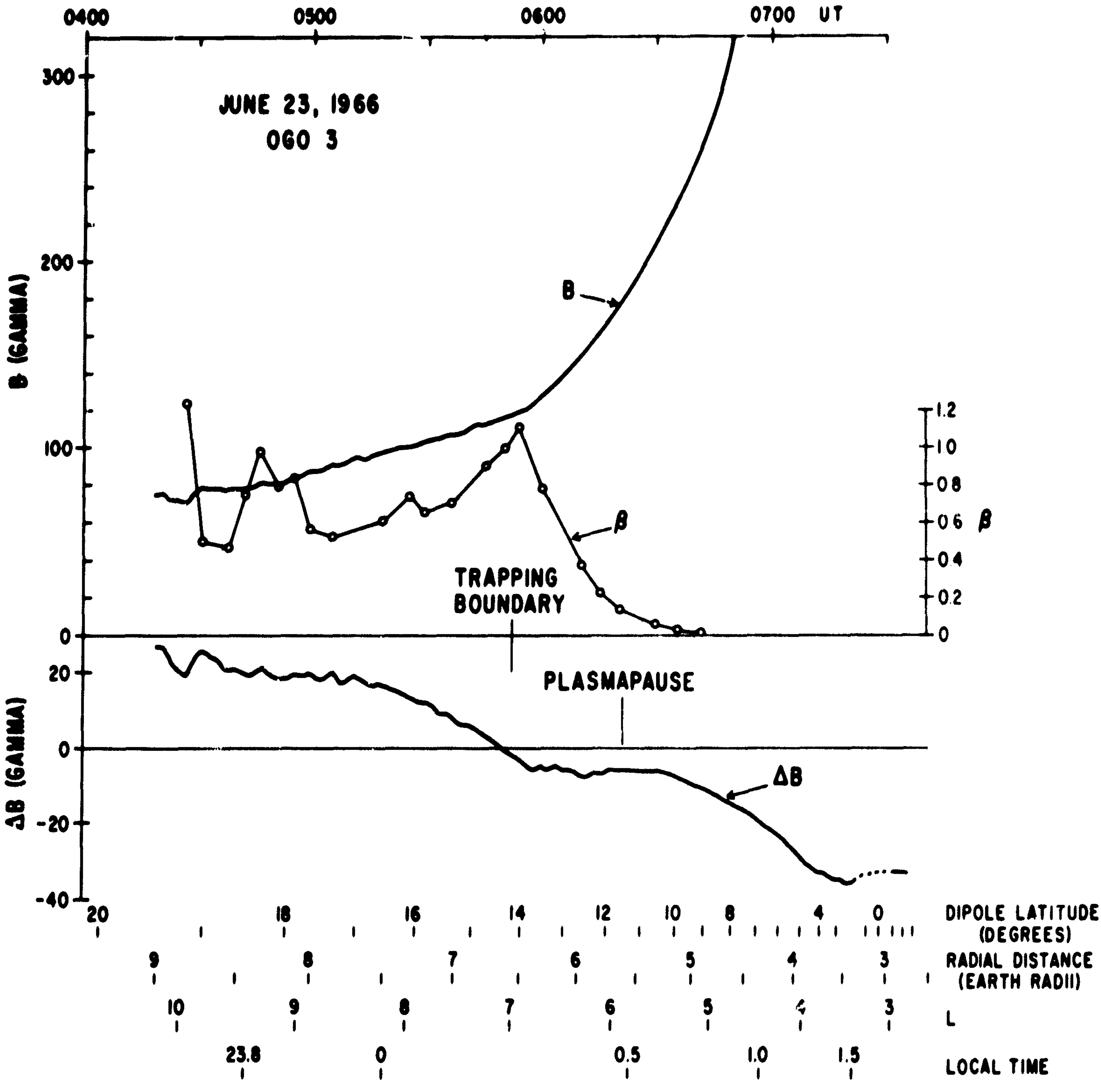

Figure 10

NASA-GSFC